EARTH REFLECTANCE SPECTRA FROM 300-1750 NM MEASURED BY SCIAMACHY

P. Stammes, J.R. Acarreta, W.H. Knap, and L.G. Tilstra
Royal Netherlands Meteorological Institute (KNMI)
P.O. Box 201, 3730 AE, De Bilt, The Netherlands

ABSTRACT

SCIAMACHY onboard ESA's Envisat satellite, launched in 2002, is a spectrometer covering the wavelength range 240-2380 nm with a spectral resolution between 0.2 and 1.5 nm. SCIAMACHY offers for the first time a contiguous spectral view of the Earth in the shortwave domain. Here we show some first top-of-atmosphere reflectance spectra of typical Earth scenes.

1. INTRODUCTION

Since the launch of GOME/ERS-2 in 1995, reflectance spectra of the Earth with moderately high spectral resolution of 0.2-0.4 nm have become available for the range 240-800 nm. SCIAMACHY is the successor of GOME, but with increased capabilities (Bovensmann et al., 1999). It has a much wider spectral range, including the near-infrared, and also has limb and occultation modes. SCIAMACHY is able to detect trace gases relevant to the ozone layer such as ozone and BrO, air pollution gases such as NO_2 and CO, and greenhouse gases such as H_2O, CO_2, and CH_4.

2. DESCRIPTION OF SCIAMACHY

SCIAMACHY has 8 spectral channels with diode-array detectors, having 1024 pixels per channel. Channels 1-5 cover the range 240-1000 nm, with a resolution of 0.2 to 0.5 nm, channel 6 covers the range 1000-1750 nm with a resoluton of 1.5 nm, whereas channel 7 and 8 cover the ranges 1940-2040 nm and 2265-2380 nm, with a respective resolution of 0.2 and 0.3 nm. SCIAMACHY measures both in nadir and limb, by alternatively switching its viewing mode. Here we only consider nadir data with a spatial resolution of 240×30 km^2.

SCIAMACHY observes the sun every day. Therefore, the Earth reflectance can be determined from the Earth radiance and solar irradiance measurements by SCIAMACHY. This accounts for some calibration errors, but not all. From comparison of the SCIAMACHY measured reflectances with UV radiative transfer model calculations (Tilstra et al., 2004) and with MERIS reflectances between 440 and 880 nm (Acarreta and Stammes, 2005) it appears that the SCIAMACHY reflectances are about 10-20% too low. The reason for this radiometric calibration error probably lies in the pre-flight measurements. Ad-hoc correction for this radiometric error is possible by using a reflectance correction factor, but this has not been done in the results shown hereafter.

3. OBSERVED REFLECTANCE SPECTRA

The quantity used here is the Earth's reflectance:

$$R = \pi I / (\mu_0 E),$$

where I is the radiance reflected at top-of-atmosphere (TOA), in W/m^2/sr/nm, E is the solar irradiance incident at TOA perpendicular to the beam, in W/m^2/nm, and μ_0 is the cosine of the solar zenith angle. We focus on SCIAMACHY channels 2-6, i.e. the spectral range 300-1750 nm, because channels 1, 7 and 8 currently suffer from dark current problems.

We have selected five typical Earth scenes from Envisat orbit 2509, 23 August 2002: cloud-free ocean, cloud-free Sahara desert, cloud-free vegetated land, thick water clouds, and thick ice clouds. Scenes were selected using colocated images from MERIS, which is also onboard Envisat. See Figs. 1-3 for the spectra, which are discussed below. Note that the spectra are split into two parts: 300-800 nm and 800-1800 nm.

3.1 Ocean scene (Figure 1)

At UV and visible wavelengths the cloud-free ocean reflectance is dominated by atmospheric Rayleigh scattering. The combination of Rayleigh scattering and ozone absorption causes the characteristic peak in the reflectance around 330 nm, with a value of about 0.3. At 800 nm the reflectance in the continuum is only 0.02, and at 1750 nm only 0.01. Since water itself is almost black beyond 700 nm, this reflectance is due to aerosol and Rayleigh scattering, with possibly contributions from the ocean surface (glitter, white caps).

3.2 Land scenes (Figure 2)

Also the reflectances of the cloud-free land scenes contain the Rayleigh peak at 330 nm. The Sahara spectrum is dominated by the steadily rising continuum reflectance beyond 500 nm, which attains a value of almost 0.6 at 1700 nm. The vegetation spectrum shows a

IRS 2004: Current Problems in Atmospheric Radiation
Fischer and Sohn (Eds.)

ISBN 0-937194-49-2

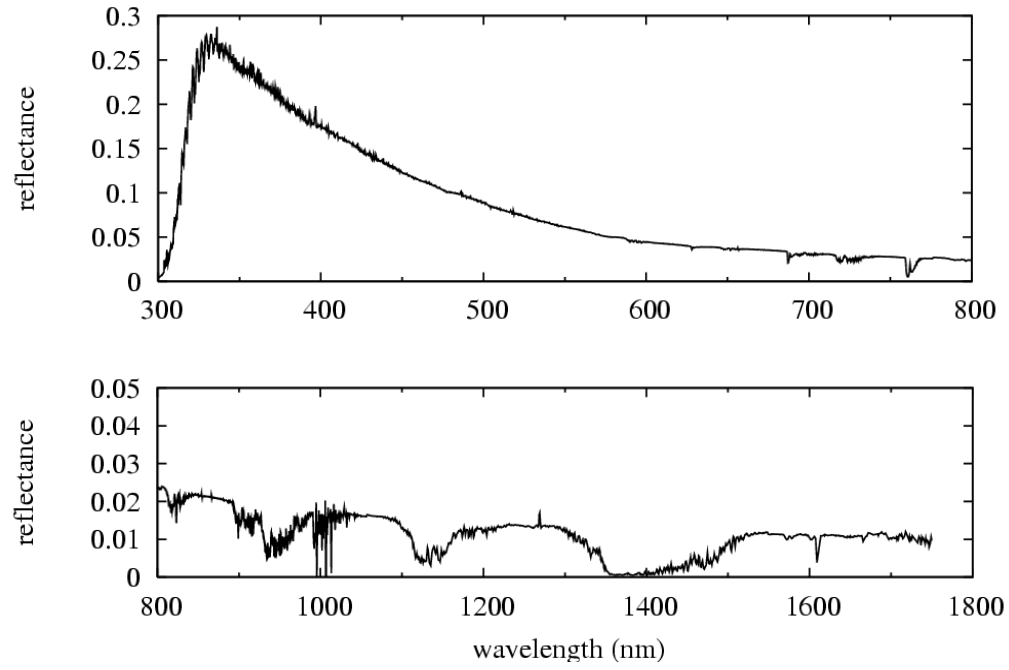

Fig. 1. SCIAMACHY nadir reflectance spectrum of a cloud-free ocean scene (45.2° N, 4.4° W), with $\mu_0 = 0.77$.

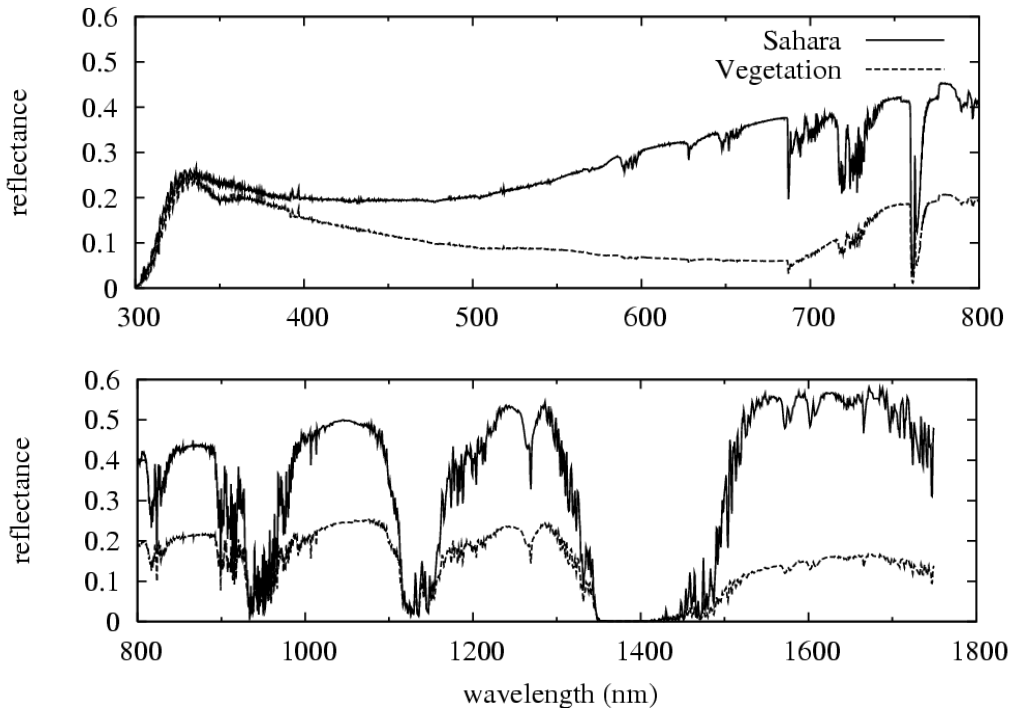

Fig. 2. SCIAMACHY nadir reflectance spectra of cloud-free land scenes: Sahara desert (31.1° N, 17.3° E) and vegetated land (53.9° N, 28.6° E). Here $\mu 0 = 0.87$ for desert and 0.74 for vegetation.

decreasing behaviour from 330 to 700 nm, except for a weak bump from 500-600 nm, which gives the green colour to vegetation. From 700-750 nm a steep rise of the reflectance occurs, which is known as the red edge. The vegetation reflectance remains about 0.2 from 800 to 1300 nm, and then decreases. Both land spectra show strong gaseous absorption bands beyond 700 nm (cf. Sect. 4).

ISBN 0-937194-49-2

3.3 Clouds (Figure 3)

The cloud spectra shown in Fig. 3 were chosen as being representative of optically thick clouds. The ice cloud spectrum and water cloud spectrum have a very similar behaviour from 300 to about 1200 nm. In that range the continuum reflectance is almost constant with wavelength. However, large differences between water and ice clouds occur from 1500 to 1750 nm. There ice clouds absorb more than water clouds, and have a different absorption spectrum.

This is due to the different refractive index of water and ice, and to the larger size of ice particles (Knap et al., 2002; Acarreta et al., 2004). The H_2O bands in the ice cloud spectrum are weaker than in the water cloud spectrum, due to the higher altitude of ice clouds.

4. COMPARISON WITH MODTRAN

To verify the atmospheric absorption bands in the SCIAMACHY spectra, we simulated a clear-sky reflectance spectrum with the MODTRAN4 radiative transfer model (version 1.1, Berk et al., 2000). We chose a triangular slit function chosen for the MODTRAN calculations with a FWHM of 10 cm^{-1}. This resolution is comparable to that of SCIAMACHY. The step size chosen was 5 cm^{-1}. In MODTRAN multiple scattering was included according to the 8-streams DISORT option. The atmospheric composition was that of the Midlatitude Summer standard atmosphere. No clouds or aerosols were included.

Figure 4 shows the calculated nadir reflectance for a clear sky case with surface albedo 0.50. In this figure the major gaseous absorption bands have been indicated. As can be seen from comparison with the SCIAMACHY spectra, most easily with that of water clouds, the absorption bands of O_3, H_2O, O_2, CO_2, and CH_4 are indeed well reproduced by MODTRAN. However, some absorption bands, e.g., due to NO_2 around 425 nm and O_2-O_2 at 477 nm and 570 nm, are missing in the MODTRAN simulation. Furthermore, the numerous small peaks in the UV and visible parts of the SCIAMACHY spectra, which are due to the Ring effect (rotational Raman scattering in the atmosphere), are not found in the MODTRAN simulations. From the comparison with the MODTRAN spectrum, it also appears that there are calibration errors in the SCIAMACHY spectra, which appear as jumps at the channel overlaps at 400 nm, 780 nm, and 1000 nm.

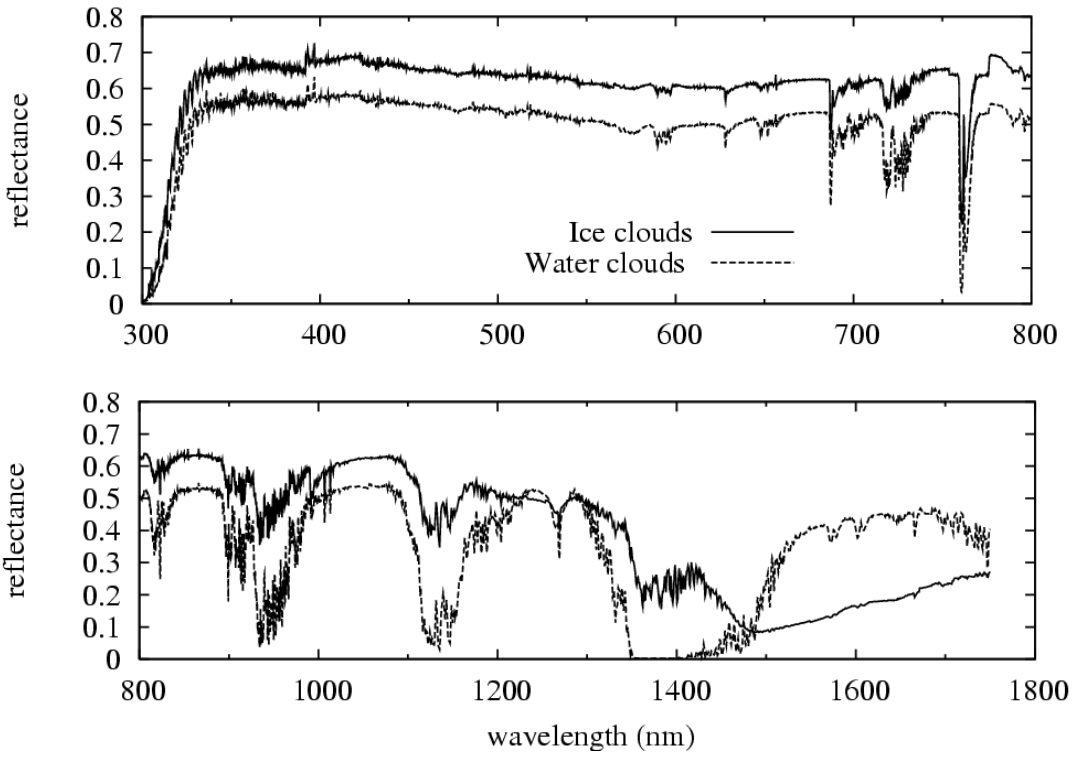

Fig. 2. SCIAMACHY nadir reflectance spectra observed over optically thick water and ice clouds: water clouds (60.1° N, 2.7° W) and ice clouds (14.8° N, 15.4° W). Here μ_0 = 0.64 for the water clouds and 0.86 for the ice clouds.

ISBN 0-937194-49-2

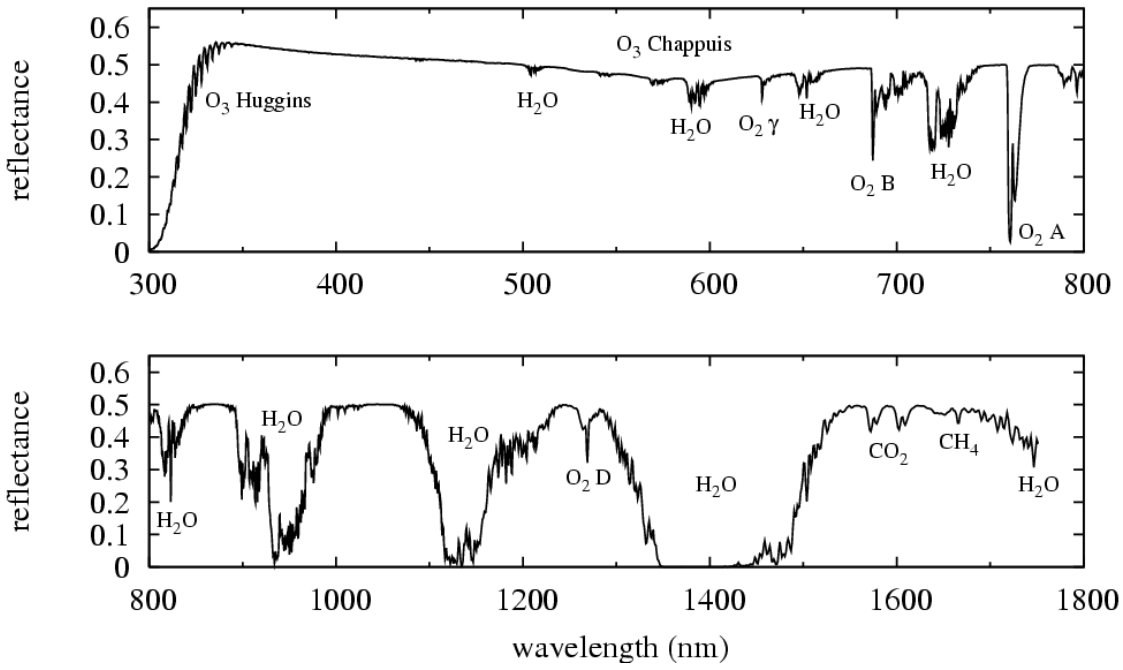

Fig. 3. MODTRAN4 simulation of nadir reflectance of a clear scene with surface albedo 0.50; $\mu_0 = 0.87$.

ACKNOWLEDGEMENTS

We are glad to acknowledge the assistance of Ankie Piters (KNMI) and the personnel of the Netherlands SCIA-MACHY Data Center (http://neonet.knmi.nl/neoaf) in making the SCIAMACHY data accessible. SCIAMACHY data have been provided by ESA/DLR. The Modtran models have been kindly provided by G. Anderson and A. Berk (Air Force Research Lab, Hanscom, MA).

REFERENCES

Acarreta, J.R., P. Stammes, and W.H. Knap, "First retrieval of cloud phase from SCIAMACHY spectra around 1.6 micron", *Atmos. Res*., Vol. 72, 89-105 (2004).

Acarreta, J.R., and P. Stammes, 2005, "Calibration comparison between SCIAMACHY and MERIS on board ENVISAT", *IEEE Geoscience and Remote Sensing Letters (GRSL),* vol. **2**, 31-35, doi: 10.1109/LGRS.2004.838348.

Berk, A., et al., "MODTRAN4 user's manual", 1 June 1999 (Last revised 17 April 2000), Air Force Research Laboratory, Hanscom AFB, MA.

Bovensmann, H., J.P. Burrows, M. Buchwitz, J. Frerick, S. Noël, V.V. Rozanov, K.V. Chance, and A.P.H. Goede, 1999: "SCIAMACHY: mission objectives and measurement modes", *J. Atmos. Sci.* **56**, 127-150.

Knap, W. H., P. Stammes, R. B. A. Koelemeijer, "Cloud thermodynamic phase determination from near-infrared spectra of reflected sunlight", *J. Atmos. Sci.,* **59**, 83-96 (2002).

Tilstra, L.G., G. van Soest, M. de Graaf, J.R. Acarreta, and P. Stammes, "Reflectance comparison between SCIAMACHY and a radiative transfer code in the UV", In: *Envisat Validation Workshop Proceedings (ACVE-2),* ESA Special Publication SP-562, May 3-7, 2004, Frascati, Italy.

ISBN 0-937194-49-2